J. Math. Biology 7, 339–352 (1979)

Journal of Mathematical Biology

A Simple Model for Phase Locking of Biological Oscillators

Leon Glass and Michael C. Mackey

Department of Physiology, McGill University, 3655 Drummond Street, Montreal, Quebec, H3G 1Y6, Canada

Summary. A mathematical model is presented for phase locking of a biological oscillator to a sinusoidal stimulus. Analytical, numerical and topological considerations are used to discuss the patterns of phase locking as a function of the amplitude of the sinusoidal stimulus and the relative frequencies of the oscillator and the sinusoidal stimulus. The sorts of experimental data which are needed to make comparisons between theory and experiment are discussed.

I. Introduction

One of the simplest models for biological oscillators assumes that a variable of interest, which we call the activity, increases linearly with time until it reaches a threshold. Once the threshold is reached the activity instantaneously and discontinuously resets to zero and the process repeats. Despite the oversimplifications inherent in this model, it has been of heuristic value in neurobiology (the 'integrate and fire' model) (Rescigno et al., 1970; Stein et al., 1972; Knight, 1972a, b; Fohlmeister et al., 1974; Hartline, 1976) and cell biology (the 'mitogen' model) (Sachsenmaier et al., 1972; Kauffman, 1974; Tyson and Sachsenmaier, 1978).

In the following, we show that if the threshold is sinusoidally modulated in time, the oscillator may become synchronized to the sinusoidal stimulus so that the activity reaches threshold at definite fixed phases of the sinusoidal threshold modulation. If in the synchronized mode the frequency of the modulation and the oscillator are in a ratio of N:M, we say that the system displays N:M phase locking. Figure 1 illustrates several phase locking patterns for this model.

Phase locking of biological oscillators to sinusoidal inputs[1] has been observed in a

[1] We do not consider the synchronization of biological oscillators to periodic pulsed inputs. Extensive references to experimental and theoretical papers dealing with this problem can be found in Hartline (1976), Stein (1977) and Winfree (1977).

0303-6812/79/0007/0339/$02.80

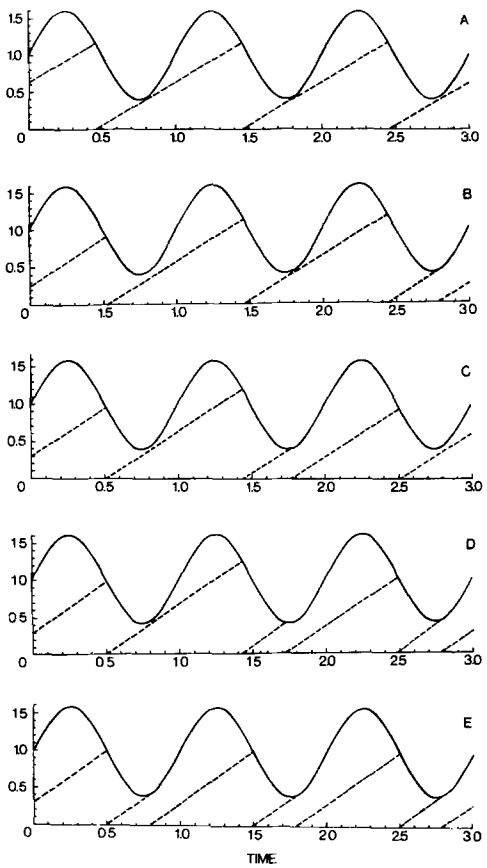

Fig. 1. Phase locking patterns for the integrate and fire model with sinusoidal threshold modulation. The dashed line represents the activity and the solid line the threshold. The parameter λ^{-1} which is defined in the text in Section 2, represents the ratio of the frequency of the sinusoidal stimulus, to the natural frequency of the unperturbed oscillator. (A) 1:1 phase locking, $\ln \lambda^{-1} = -0.16$; (B) 3:4 phase locking, $\ln \lambda^{-1} = -0.20$; (C) 2:3 phase locking, $\ln \lambda^{-1} = -0.24$; (D) 3:5 phase locking, $\ln \lambda^{-1} = -0.32$; (E) 1:2 phase locking, $\ln \lambda^{-1} = -0.36$

large number of biological preparations, e.g., cardiac rhythms in the cat can be synchronized to sinusoidal vagal stimulation (Reid, 1969) and central oscillations in ganglia controlling flying in locusts can be synchronized to sinusoidal wing flapping (Wendler, 1974).

One obstacle to quantitative work on phase-locking is the difficulty encountered in the analysis of phase locking of nonlinear oscillations to sinusoidal stimuli. Thus, despite several decades of work (Cartwright and Littlewood, 1951; Hayashi, 1964; Grasman et al., 1976) a complete understanding of phase locking of the van der Pol oscillator to sinusoidal inputs seems distant, and recent work has emphasized a numerical approach (Flaherty and Hoppensteadt, 1978).

These difficulties have led a number of investigators to consider simple integrate and fire models for phase locking (Rescigno et al., 1970; Stein et al., 1972; Knight, 1972a). In these studies activity is an integral of a sinusoidal input and the threshold is constant. Where experimental results were available for comparison, there has been good agreement with the theoretical predictions (Knight, 1972b; Fohlmeister et al., 1974).

To the best of our knowledge there have been no previous studies of the effects of threshold modulation in integrate and fire models. We have been led to consider this possibility as a consequence of experimental studies of respiratory phase locking to an artificial ventilator currently underway in our laboratory. In the mammalian respiratory system there is good experimental evidence that the degree of lung inflation acts to modulate the threshold of the 'inspiratory off-switch' (Clark and von Euler, 1972; Wyman, 1977). Moreover, we believe that in other systems in which the mechanism of phase locking is not well understood (Reid, 1969; Van der Tweel et al., 1973; Wendler, 1974) threshold modulation may well play an important role.

The model is presented in Section II, and in Section III the zones for N:1 phase locking are computed. In Section IV we show that the phase locking properties of the model reduce to an analysis of certain one-dimensional maps, the Poincaré maps. Numerical computations of the Poincaré maps have been performed to determine the phase locking regimes and to compute the stability of the phase locking computed in Section III. The results are discussed in Section V. In the Appendix we discuss topological aspects of the Poincaré maps.

II. A Mathematical Model for Phase Locking

The linearly increasing activity is $X(T)$, and the sinusoidally modulated threshold is $\Theta(T)$, where for $T = 0$, $0 \leqslant X(0) < \Theta(0)$. The activity is

$$X(T) = X(0) + \Lambda T, \quad T \geqslant 0 \tag{1}$$

where Λ is a positive constant. The modulated threshold is

$$\Theta(T) = \Theta_0 + K \sin(\omega T + \phi), \quad 0 \leqslant K < \Theta_0 \tag{2}$$

where $\Theta_0 > 0$ is the mean threshold, $\omega > 0$ is the angular frequency of the sinusoidal modulation, $\phi > 0$ is the phase of the sinusoidal modulation, and $K \geqslant 0$ is the amplitude of the threshold modulation function. The activity will increase until it reaches the threshold, and reset to zero. The time T' when the activity first reaches threshold is found by equating the right hand sides of (1) and (2) and solving for the smallest root satisfying the criterion $T' > 0$. Since $X(0) < \Theta(0)$, the root must exist. For $T \geqslant T'$ the activity is

$$X(T) = \Lambda(T - T'). \tag{3}$$

The right hand sides of (2) and (3) are equated to compute the second time T'' when activity reaches threshold, and so forth.

Analytical and numerical computations are facilitated by rescaling (1) and (2). Dimensionless parameters and variables are designated by lower case letters. Defining

$$\begin{aligned} t &= \omega T/2\pi \\ x(t) &= X(T)/\Theta_0 \qquad k = K/\Theta_0 \\ \theta(t) &= \Theta(T)/\Theta_0 \qquad \lambda = 2\pi\Lambda/\omega\Theta_0 \end{aligned} \tag{4}$$

(1) and (2) become

$$x(t) = x(0) + \lambda t, \qquad t \geqslant 0, \tag{5}$$

$$\theta(t) = 1 + k \sin(2\pi t + \phi), \quad 0 \leqslant k < 1. \tag{6}$$

Note that in (5) and (6) the period and the mean amplitude of the sinusoidal modulation have been set equal to 1. In (1) and (2), as well as (5) and (6), the ratio of the frequency of the sinusoidal modulation to the frequency of the unperturbed oscillator ($K = k = 0$) is given by $\lambda^{-1} = (\omega\Theta_0/2\pi\Lambda)$.

In the remainder of this article we discuss the behavior of the model described by (5) and (6) in (λ, k) parameter space. We consider the behavior for all possible initial conditions by setting $\phi = 0$ and considering $x_0 \varepsilon [0, 1)$.

III. N:1 Phase Locking

Here we compute criteria for the existence of N:1 phase locking. Assume that at some time $t_i \varepsilon [0, 1)$, $x(t_i) = 0$. Then to have N:1 phase locking it is necessary that

$$\begin{aligned} N\lambda &= 1 + k \sin 2\pi(t_i + N) \\ &= 1 + k \sin 2\pi t_i. \end{aligned} \tag{7}$$

Equation (7) can be used to compute t_i. In order to have real solutions to (7),

$$k \geqslant |\lambda N - 1| \tag{8}$$

must be satisfied. If the inequality in (8) holds there will be two roots for (7), and for the equality there will be one root. The two roots will be designated t_s and t_u. As we show below, the subscript s refers to a stable solution (the phase locked solution) whereas the subscript u refers to an unstable solution. Define

$$\alpha = \frac{1}{2\pi} \sin^{-1} \frac{|\lambda N - 1|}{k}, \quad 0 \leqslant \alpha \leqslant \tfrac{1}{4} \tag{9}$$

so for the case $\lambda N \geqslant 1$,

$$t_u = \alpha, \qquad t_s = \tfrac{1}{2} - \alpha \tag{10}$$

and for the case $\lambda N < 1$

$$t_u = 1 - \alpha, \qquad t_s = \tfrac{1}{2} + \alpha. \tag{11}$$

Note that for $|\lambda N - 1| = k$, $\alpha = \frac{1}{4}$ and the two roots coalesce.

In order for a solution of (7) to be meaningful, the activity must be less than the threshold resetting curve for all times $t \varepsilon (t_i, t_i + N)$. Setting

$$g(t, t_i) = 1 + k \sin 2\pi t - \lambda(t - t_i), \tag{12}$$

we must have

$$g(t, t_i) > 0 \quad \text{for } t \varepsilon (t_i, t_i + N). \tag{13}$$

Differentiating (12) determines the time, $t_{\min}$, when $g(t, t_i)$ is a minimum. For $\lambda > 2\pi k$, $t_{\min} = t_i + N$. Consequently, for this situation both solutions t_s, t_u in (10)

and (11) are physically meaningful. However, for $\lambda \leqslant 2\pi k$ a different situation holds. If

$$\beta = \frac{1}{2\pi} \cos^{-1} \frac{\lambda}{2\pi k}, \quad 0 \leqslant \beta \leqslant \tfrac{1}{4}, \tag{14}$$

the first derivative is zero for $t = \beta, 1 \pm \beta, 2 \pm \beta, \ldots$. However, the restriction that $t_{\min} \varepsilon (t_i, t_i + N]$, along with a consideration of the second derivative of (12), gives $t_{\min}$ as

$$t_{\min} = N - \beta, \quad t_i \leqslant 1 - \beta, \tag{15}$$

$$t_{\min} = N + 1 - \beta, \quad t_i > 1 - \beta, \tag{16}$$

where t_i is computed from (10) or (11). Equation (16) is required for computations of the root t_u from (11).

The equations developed in this section were used to numerically compute the N:1 phase locking zones. For fixed values of k and N, (8) determines a possible range for λ. Values for λ in this range are selected and, using either (10) or (11), t_s and t_u are computed. Then using (12)–(16) we determine whether there are zero, one, or two allowable solutions.

The results are shown in Fig. 2. The boundaries of N:1 phase locking regimes are thin solid lines. The boundaries separating the regions in which there are one or two

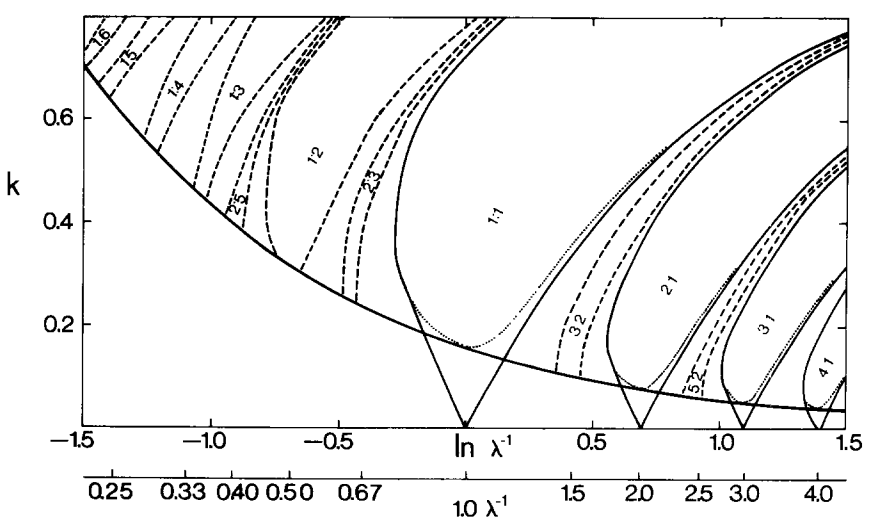

Fig. 2. Phase locking patterns in (λ, k) parameter space. The borders of the N:1 locking patterns, indicated by thin solid lines were computed in Section 3, and the borders of the other locking regions are indicated by dashed lines, computed in Section 4. In the N:1 locking regions the dotted lines separate the regions in which there is one solution (above the dotted lines) from the regions in which there are two solutions (beneath the dotted lines), see Section 3. The dotted lines asymptotically approach the right hand boundaries of the N:1 regions. The thick solid line $\lambda = 2\pi k$ separates Region 1 (above the line) from Region 2 (beneath the line). The behavior in these two Regions is discussed in Section 4 and the Appendix

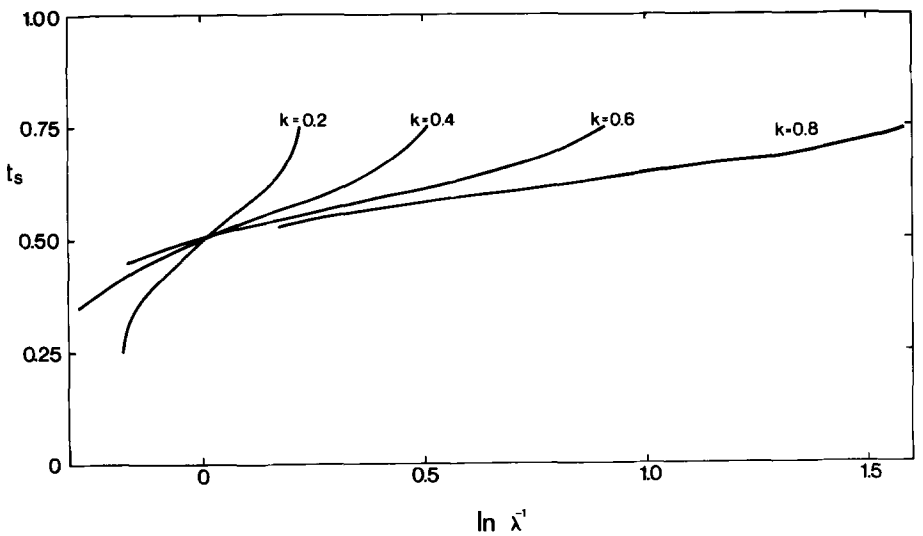

Fig. 3. The phase of the stable phase locked solution, t_s, as a function of λ for several values of k in the 1:1 phase locking region

stable solutions are dotted lines. In all cases, the regions in which there is one solution are above the dotted lines, while regions in which there are two solutions are beneath the dotted lines. For the case in which there is one solution, this solution is stable and corresponds to the phase t_s computed from (10) or (11).

One of the experimental observables in a phase locking experiment is the relative phase of the oscillator and the driving stimulus. In Fig. 3 we give t_s as a function of $\ln \lambda^{-1}$ for several values of the amplitude of the sinusoidal modulation.

IV. The Poincaré Map

Consider the mathematical model for phase-locking described by (5) and (6) with $\phi = 0$. Let the value of $x(t)$ at $t = j$ be x_j ($j = 0, 1, 2, \ldots$). For an initial condition $x_0 \varepsilon [0, 1)$ we have $x_j \varepsilon [0, 1)$ for $j = 1, 2, \ldots$. The model defines a transformation T such that

$$\begin{aligned} x_{j+1} &= Tx_j \\ x_{j+2} &= T(Tx_j) = T^2(x_j) \\ x_{j+N} &= T(T^{N-1}x_j) = T^N(x_j). \end{aligned} \tag{17}$$

The transformation T is referred to as the Poincaré, or phase advance, map (Cartwright and Littlewood, 1951; Arnold, 1973; Flaherty and Hoppensteadt, 1978).

A fixed point P of T of period N is defined by

$$\begin{aligned} &T^N(P) = P \\ &T^i(P) \neq P, \quad i = 1, \ldots, N-1. \end{aligned} \tag{18}$$

A fixed point P of period N will correspond to a solution exactly synchronized to the sinusoidal modulation and which repeats with a periodicity of N.

Here the Poincaré maps have been used to: (a) compute the stability of the N:1 locking patterns determined in Section III; and (b) compute boundaries in (λ, k) space for several other phase locking patterns. The topological properties of the Poincaré maps are discussed in the Appendix.

A. Stability of N:1 Locking

Assume that there is a fixed point P, satisfying (18), corresponding to a root t_i $(i = u, s)$ computed from (10) or (11). The first derivative of the period N Poincaré map computed at P, designated $(T^N)'_P$, is defined by

$$(T^N)'_P = \lim_{\delta \to 0} \frac{T^N(P + \delta) - T^N(P)}{\delta}. \tag{19}$$

If $|(T^N)'_P| < 1$ the solution is locally stable and if $|(T^N)'_P| > 1$ the solution is locally unstable. Calling $m = (d\theta/dt)_{t=t_i}$ we compute

$$(T^N)'_P = \frac{\lambda}{\lambda - m}. \tag{20}$$

Since $\lambda \geqslant m$, if the slope of the threshold modulation curves is positive at the time threshold is reached in an N:1 pattern, the solution will be locally unstable; if the slope is negative, the solution will be locally stable. This justifies the use of the subscripts in (10) and (11). There is a singular case corresponding to the solution $t_s = t_u = \frac{1}{4}$, $t_s = t_u = \frac{3}{4}$. This only occurs at the boundaries of the N:1 phase locking regimes where the equality (8) is satisfied. In this case $m = 0$ and the solutions are semistable. An extensive discussion of this situation is found in Arnold (1965). These analytical computations consider only the local stability of the periodic solutions, while the numerical studies described below suggest that locally stable solutions are globally stable (except perhaps for a set of measure zero).

B. Numerical Studies in (λ, k) Parameter Space

We have numerically computed the Poincaré map at a large number of points in the (λ, k) space. Initial studies sampled (λ, k) space on a coarse grid of approximately 100 points covering the region shown in Fig. 2. In this region the ratio of perturbation to natural frequency varies over a range of approximately 1:4 to 4:1. We computed $T^N(x)$ where $N = 1, 2, 3, 4$.

On this coarse grid, the studies indicated that (λ, k) parameter space was separated into two regions. In the lower left corner (Fig. 2), we did not, in general, locate fixed points for the Poincaré maps, whereas in the remainder of parameter space practically all points showed fixed points of low periodicity. Subsequent considerations have led us to consider the dividing line between these two regions as

the curve $\lambda = 2\pi k$ (the heavy black line in Fig. 2). We consider the behavior in the two regions separately.

Region 1. $\lambda < 2\pi k$. Here an effort was made to determine phase locking behavior and to identify the boundaries for several phase locking regions, as determined from the Poincaré maps. In Fig. 4 we show the Poincaré maps $T^N(x)$, $N = 1, 2, 3$, for five values of λ corresponding to the phase locking patterns shown in Fig. 1. Consider the case where $\ln \lambda^{-1} = -0.16$. Note that $T(P_0) = P_0$ for $P_0 \cong 0.64$. Under iteration of T all points are attracted to P_0 and no new fixed points arise. Consequently for this case the 1:1 phase locking pattern shown in Fig. 1 is globally stable since all initial values of the activity approach the cycle. For the other cases shown in Fig. 1, analysis of the associated numerically computed Poincaré maps (Fig. 4) shows that the phase locked patterns are globally stable.

The boundaries for several phase locking regions have been numerically determined by examining the Poincaré maps for points in the (λ, k) plane between points of known behavior. Such methods are necessarily approximate. Numerical computation of the N:1 phase locking regions were completed prior to the analytical studies of Section III, and indicate that the localization of boundaries is accurate to at least ± 0.05 log units on the abscissa.

However, numerical studies at a large number (more than 200) points in (λ, k) space have successfully identified globally stable phase locking patterns in practically all cases. Although most points showed phase locking in comparatively simple patterns, as shown in Fig. 2, attempts to dissect the boundaries between any two neighboring regions always revealed new phase locking patterns. In Table 1 we give phase locking patterns observed in the region between the 1:1 and 2:3 phase locking. Note that for k constant, as λ^{-1} decreases, the phase locking patterns form a decreasing sequence of rational ratios. Further numerical studies would be expected to show new phase locking patterns intercalated between those shown in Table 1 as λ^{-1} is probed on a finer grid. However, in view of the comparatively small volume of (λ, k) space occupied by higher order phase locking patterns, we have not included them in Fig. 2. In the Appendix, we return to the question of phase locking behavior in Region 1.

Region 2. $\lambda \geqslant 2\pi k$. Sampling points in (λ, k) space on a coarse grid gave few points which showed phase locking after a few iterations of the Poincaré map. However, on theoretical grounds (see Appendix) we know that all possible N:M phase locking patterns are found in this region. Consequently, it appears that the relative volume of (λ, k) space occupied by low period phase locking patterns is small in Region 2 compared to Region 1. The computations in Section 3 show a 'funneling' of the N:1 phase locking regions in Region 2.

The numerical difficulties involved in localizing boundaries in Region 2 can be illustrated by an example. An attempt was made to localize the boundaries of the 2:5 phase locking region for $k = 0.03$. For this value of k the entire 2:5 region

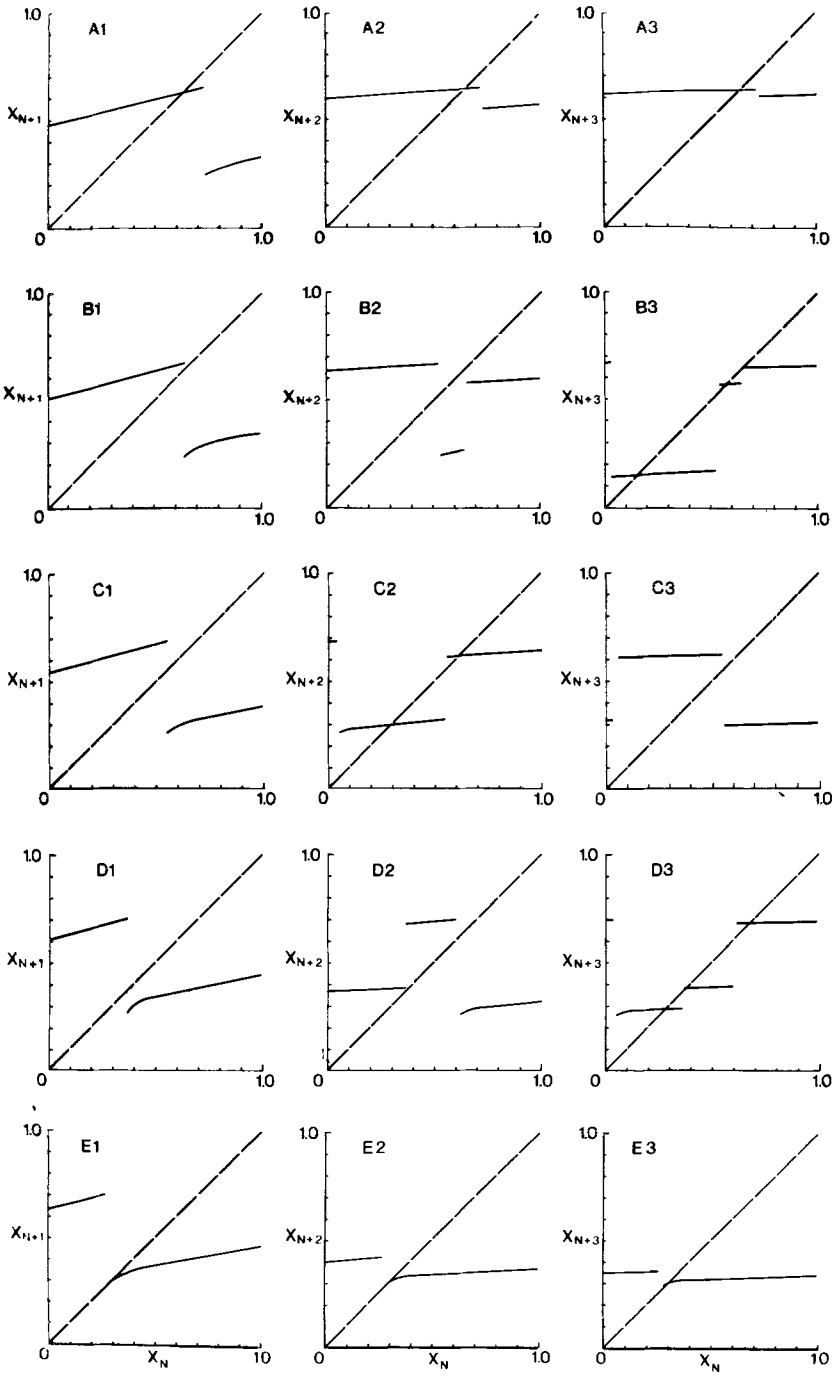

Fig. 4. Numerically computed Poincaré maps for the phase locking patterns shown in Fig. 1. (A) $\ln \lambda^{-1} = -0.16$; (B) $\ln \lambda^{-1} = -0.20$; (C) $\ln \lambda^{-1} = -0.24$; (D) $\ln \lambda^{-1} = -0.32$; (E) $\ln \lambda^{-1} = -0.36$

Table 1. Phase locking patterns observed for several values of k and λ

k	$\ln \lambda^{-1}$	Phase locking
0.3	−0.20	1: 1
	−0.30	13:16
	−0.35	3: 4
	−0.40	15:22
	−0.45	2: 3
0.4	−0.28	1: 1
	−0.30	5: 6
	−0.32	3: 4
	−0.36	5: 7
	−0.44	2: 3
0.6	−0.187	1: 1
	−0.188	6: 7
	−0.189	5: 6
	−0.190	4: 5
	−0.200	3: 4
	−0.240	2: 3
0.8	0.16000	1: 1
	0.15000	3: 4
	0.14439	5: 7
	0.14438	7:10
	0.14420	9:13
	0.14418	11:16
	0.14416	2: 3

occurs within the range $-0.91611 < \ln \lambda^{-1} < -0.91610$, where the limits lie outside the 2:5 locking region.

In view of the small volume of (λ, k) space occupied by phase locking patterns of low period and the resulting numerical difficulties involved in locating the boundaries, but the theoretical certainty that the phase locked regions exist, we have not localized the boundaries in Region 2.

V. Discussion

The results presented here pose sharp problems for both mathematicians and biologists.

There is a rich and interesting mathematical literature dealing with the properties of the Poincaré maps for our simple model (Appendix). It will be of interest if the properties of this simple model for phase locking are preserved in models for which the oscillator is given as a nonlinear differential equation in two or more dimensions. In this context, it is common to consider the integrate and fire model as an approximation of an 'extreme relaxation oscillator' in which the time scale for the descending phase is very much more rapid than the time scale for the ascending phase. However, caution in interpretation is certainly needed since the topological

properties of the Poincaré maps in one dimension depend critically on whether the map is discontinuous or continuous. For example, the discontinuities in the Poincaré maps (see Fig. 4) contradict the hypotheses of the Li–Yorke theorem which would otherwise be applicable to at least some of the (λ, k) parameter space (Li and Yorke, 1975).

Since nonlinear oscillators are expected to phase lock to periodic stimuli, the observation of phase locking alone can do little to elucidate the mechanism of the biological oscillator or the coupling between the oscillator and the external perturbation. In Figs. 2 and 3 we have given quantitative predictions for the phase locking patterns and phase angles for a mathematical model of phase locking. Although our model is consistent with qualitative observations concerning phase locking in experimental preparations (Reid, 1969; Van der Tweel et al., 1973) detailed quantitative data concerning the pattern of phase locking over a range of frequencies and amplitudes of the external stimuli will be needed before comparisons can be made between experimental and theoretical studies.

Appendix

Topological Considerations

Here the points $x_j = 0$ and $x_j = 1$ can be identified since we have assumed that the activity resets to zero instantaneously. Thus, the Poincaré map T can be thought of as one which takes the unit circle into itself.

In (λ, k) parameter space there are two regions for the Poincaré map. First, note that T is always one-one since distinct elements are carried into distinct elements.

Region 2. $\lambda \geqslant 2\pi k$

Here the maximum slope of the threshold modulation curve is less than or equal to the slope of the linearly increasing activity. The range and codomain of the transformation T are equal and T is a one-one map of the unit circle *onto* itself. T is continuous and differentiable on the unit circle.

Region 1. $\lambda < 2\pi k$

Here the range and codomain of T are no longer equal, so T is a one-one map of the unit circle *into* itself. T is monotonic, piecewise continuous, and piecewise differentiable (Fig. 4).

Topological Considerations – Region 2. The class of maps which arise in Region 2 have been subjected to extensive analysis (Denjoy, 1932; Coddington and Levinson, 1955; Peixoto, 1960; Arnold, 1965; Rosenberg, 1977). We are not competent to review this work in detail, but wish to draw attention to certain results which are of interest in the current context. Our presentation follows Knight (1972a).

If T is a continuous differentiable one-one map of the unit circle onto itself, then a 'rotation number' or 'turning angle' $\alpha(T)$ defined by

$$\alpha(T) = \lim_{N \to \infty} \frac{1}{N} T^N(X)$$

can be associated with T. If T depends continuously on a parameter (e.g. λ in the present case), then the turning angle also depends continuously on that parameter. Thus, rational and irrational rotation numbers are found. If $\alpha(T)$ is irrational, then T is topologically equivalent to a rigid rotation of the unit circle. If $\alpha(T)$ is rational, say m/i then either every point x of $T^i(x)$ is a fixed point, or $T^i(x)$ has a discrete set of fixed points. As noted above, if $T^i(x)$ has a discrete set of fixed points this corresponds to phase locking of the oscillator.

Let $S_I(S_R)$ be the set of points in (λ, k) parameter space in Region 2 which have an irrational (rational) turning number. It has been shown that S_R is an open dense set so that systems with rational turning numbers are structurally stable (Peixoto, 1960; Arnold, 1965). However, the measure of S_I is positive (Herman, 1977). In fact, Arnold (1965) has examined a class of maps corresponding to a rigid rotation plus a small perturbation and has shown that in the limit as the perturbation approaches zero, the measure of maps with irrational turning numbers approaches 1. The general question of the relative measures of sets with rational and irrational turning numbers as one moves around in (λ, k) parameter space appears difficult (Rosenberg, 1977; Guckenheimer et al., 1977).

Topological Considerations – Region 1. After the work reported here was completed, we became aware of other work (Keener, 1978) which treats the class of maps arising in Region 1. We briefly describe Keener's results.

For the discontinuous maps in Region 1, Keener defines the rotation number to be the average occupation time on one of the branches of the map T. The rotation number is rational if and only if some fixed iterate of T has a fixed point. If the map T depends on a parameter (e.g. λ in the present case), as the parameter is varied the rotation number will be rational everywhere except on a Cantor set of measure zero. Further, for the cases in which the rotation number is irrational, the invariant set of T is a Cantor set.

Our numerical studies show that in Region 1, the predominant behavior is phase locking in comparatively simple patterns (Fig. 2). In the regions between these simple patterns, there is stable phase locking of high periodicity (Table 1). Although there are also irregular dynamics supported on a Cantor set of measure zero in parameter space, this behavior cannot be observed in numerical simulations. However, in any real physical or biological system there will be small fluctuations in activity and threshold due to noise. Consequently we anticipate that near phase locking boundaries, and in regions of parameter space in which the rotation number is changing rapidly, the dynamics in experimental systems may be quite as irregular as the dynamics on the Cantor set of measure zero in parameter space in the strictly deterministic system.

Acknowledgements. We thank W. Langford, A. Lasota and J. Yorke for helpful conversations. This research has been supported by a grant (NRC-A-0091) from the National Research Council of Canada.

References

Arnold, V. I.: Small denominators. 1. Mappings of the circumference onto itself. Trans. of The A.M.S. Series 2. **46**, 213–284 (1965)

Arnold, V. I.: Ordinary Differential Equations. Cambridge, Mass.: MIT Press, 1973

Cartwright, M. L., Littlewood, J. E.: On nonlinear differential equations of the second order. Ann. Math. **54**, 1–37 (1951)

Clark, F. J., von Euler, C.: On the regulation of depth and rate of breathing. J. Physiol. London **222**, 267–295 (1972)

Coddington, E. A., Levinson, N.: Theory of Ordinary Differential Equations, Chapter 17. New York: McGraw Hill, 1955

Denjoy, A.: Sur les courbes definies par les equations differentielle a la surface du tore. J. Math. Pures et Appl. **11**, 333–375 (1932)

Flaherty, J. E., Hoppensteadt, F. C.: Frequency entrainment of a forced van der Pol oscillator. Studies in Appl. Math. **58**, 5–15 (1978)

Fohlmeister, J. F., Poppele, R. E., Purple, R. L.: Repetitive firing: dynamic behaviour of sensory neurons reconciled with a quantitative model. J. Neurophysiol. **37**, 1213–1227 (1974)

Grasman, J., Veling, E. J. M., Willems, G. M.: Relaxation oscillations governed by a van der Pol equation with periodic forcing term. SIAM J. Appl. Math. **31**, 667–676 (1976)

Guckenheimer, J., Oster, G., Ipaktchi, A.: The dynamics of density dependent population models. J. Math. Biol. **4**, 101–147 (1977)

Hartline, D. K.: Simulation of phase-dependent pattern changes to perturbations of regular firing in crayfish stretch receptor. Brain Res. **110**, 245–257 (1976)

Hayashi, C.: Nonlinear Oscillations in Physical Systems. New York: McGraw Hill, 1964

Herman, M. R.: Mesure de Lebesque et nombre de rotation. In Lecture Notes Mathematics, #597, Geometry and Topology, pp. 271–293, Berlin: Springer-Verlag, 1977

Kauffman, S.: Measuring a mitotic oscillator: the arc discontinuity. Bull. Math. Biol. **36**, 171–182 (1974)

Keener, J. P.: Chaotic behavior in piecewise continuous difference equations. Trans. Am. Math. Soc. 1979

Knight, B. W.: Dynamics of encoding in a population of neurons. J. Gen. Physiol. **59**, 734–766 (1972a)

Knight, B. W.: The relationship between the firing rate of a single neuron and the level of activity in a population of neurons. Experimental evidence for resonant enhancement in the population response. J. Gen. Physiol. **59**, 767–778 (1972b)

Li, T.-Y., Yorke, J. A.: Period three implies chaos. Am. Math. Monthly **82**, 985–992 (1975)

Peixoto, M. M.: Structural stability on two dimensional manifolds. Topology **1**, 101–121 (1962)

Reid, J. V. O.: The cardiac pacemaker: effects of regularly spaced nervous input. Am. Heart J. **78**, 58–64 (1969)

Rescigno, A., Stein, R. B., Purple, R. L., Poppele, R. E.: A neuronal model for the discharge patterns produced by cyclic inputs. Bull. Math. Biophys. **32**, 337–353 (1970)

Rosenberg, H.: Les diffeomorphismes du cercle. Seminaire Bourbaki, 28 e annee, 1975–76, pp. 81–98, Berlin: Springer-Verlag, 1977.

Sachsenmaier, W., Remy, V., Plattner-Schobel, R.: Initiation of synchronous mitosis in *Physarum polycephalum*. Exp. Cell Res. **73**, 41–48 (1972)

Stein, P. S. G.: Application of the mathematics of coupled oscillator systems to the analysis of the neural control of locomotion. Fed. Proc. **36**, 2056–2059 (1977)

Stein, R. B., French, A. S., Holden, A. V.: The frequency response, coherence, and information capacity of two neuronal models. Biophys. J. **12**, 295–322 (1972)

Tyson, J., Sachsenmaier, W.: Is nuclear division in Physarum controlled by a continuous limit cycle oscillator? J. Theor. Biol. **73** 723–738 (1978)
Van der Tweel, L. H., Meijler, F. L., Van Capelle, F. J. L.: Synchronization of the heart. J. Appl. Physiol. **34**, 283–287 (1973)
Wendler, G.: The influence of propioceptive feedback on locust flight coordination. J. Comp. Physiol. **88**, 173–200 (1974)
Winfree, A. T.: Phase control of neural pacemakers. Science **197**, 761–763 (1977)
Wyman, R. J.: Neural generation of the breathing rhythm. Ann. Rev. Physiol. **39**, 417–448 (1977)

Received July 27/Revised October 12, 1978